

## Ionization of H(1s) near Threshold\*

J. WILLIAM MCGOWAN† AND E. M. CLARKE‡

*Gulf General Atomic Incorporated, John Jay Hopkins Laboratory for Pure and Applied Science, San Diego, California 92112*

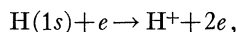
(Received 9 January 1967; revised manuscript received 18 August 1967)

An experimental study of the threshold of ionization of H(1s) has been made. The electron-impact spectrometer used has an electron-energy resolution  $\lesssim 0.06$  eV. For atomic hydrogen, it has been demonstrated that for  $\sim 0.4$  eV above threshold, the cross section for ionization is a nonlinear and complicated function of the electron energy. The form of the cross section approaches a  $(E_e - IP)^{1.13 \pm 0.03}$  power law, although within 0.05 eV of threshold a higher power law would be consistent with our data. Above 0.4 eV and for somewhat less than 3 eV, a linear law more accurately describes our result. The slope of the linear portion of the cross section is in good agreement with other experiments, but in disagreement with theory. The intercept of the linear extrapolation of the straight-line portion with the energy axis is  $0.032 \pm 0.005$  eV above threshold.

### I. INTRODUCTION

**I**n this report, we summarize results of high-resolution, electron-impact ionization studies of H while the accompanying paper gives similar results for H<sub>2</sub>. These studies have been repeated four times during the past three years under markedly differing experimental conditions.<sup>1,2</sup> The data presented here are, therefore, a compilation of results.

The intimate details of the ionization mechanism even for the simplest case



are difficult to grasp both experimentally and theoretically. A large number of theoretical studies have been made of this system,<sup>3-9</sup> but thus far no approxi-

mation for the unmanageable exact solution has been able to duplicate the magnitude of the total cross section<sup>9</sup> which has already been measured and verified a number of times.<sup>10-12</sup> In the vicinity of the ionization threshold, most of the theoretical approximations predict an energy dependence of the cross section proportional to  $(E_e - E_{IP})^n$ , where  $E_e$  is the electron energy and  $E_{IP}$  is the ionization potential. The exponent  $n$  is the predicted exponent which, depending upon the assumption chosen, is found to be either 1,<sup>3-5</sup> 1.127<sup>6</sup>, or 1.5<sup>7</sup>. The recent work of Omidvar,<sup>9</sup> however, predicts a more complex threshold law which in the threshold limit is a power law with  $n=1.5$ . Then, from  $\sim 0.06$  to  $\sim 0.6$  eV above threshold this cross section is very nearly a 1.13 power law. Above this it tends toward a higher power dependence. None of the theories can tell us over what energy interval a threshold law strictly applies. This information will have to be determined in the laboratory.

All experiments, including the present work, show that through the region  $\approx 1.0$  eV  $< (E_e - E_{IP}) < 3.0$  eV, the cross section is effectively linear. The experiments reported here extend the apparent linearity down to  $\approx 0.4$  eV, but demonstrate that the ionization-efficiency curve is nonlinear below this.

The apparatus and some of the experimental procedures described in this report have been used in other studies already reported<sup>1,2,13-15</sup> or soon to be reported.<sup>16</sup>

\* Research sponsored by NASA under Contract Nos. NAS 5-9110 and NAS 5-9321 and the Defense Atomic Support Agency.

† 1965-1966 Visiting Fellow, Joint Institute for Laboratory Astrophysics, University of Colorado, Boulder, Colo.

‡ Present address: Physics Department, St. Francis Xavier University, Antigonish, N. S.

<sup>1</sup> J. Wm. McGowan and M. A. Fineman, in *Proceedings of the Fourth International Conference on the Physics of Electronic and Atomic Collisions, Quebec, 1965*, edited by L. Kerwin and W. Fite (Science Book Crafters, Hastings-on-Hudson, New York, 1965), p. 429. The electron-energy scale must be shifted down by  $\sim 0.03$  eV in conjunction with the results of the study reported in this paper.

<sup>2</sup> (a) J. Wm. McGowan, M. A. Fineman, E. M. Clarke, and H. P. Hanson, following paper, *Phys. Rev.* **167**, 52 (1968). (b) J. W. McGowan and M. A. Fineman, *Phys. Rev. Letters* **15**, 179 (1965).

<sup>3</sup> M. R. H. Rudge and M. J. Seaton, *Proc. Roy. Soc. (London)* **A213**, 262 (1965); **83**, 680 (1964); M. R. H. Rudge and S. B. Schwartz, *ibid.* **88**, 579 (1966).

<sup>4</sup> S. Geltman, *Phys. Rev.* **102**, 171 (1956).

<sup>5</sup> R. K. Peterkop, *Izv. Akad. Nauk. Latv. S.S.R.* **9**, 79 (1960); **27**, 1012 (1963); *Proc. Phys. Soc. (London)* **A77**, 1220 (1961); *Zh. Eksperim. i Teor. Fiz.* **41**, 1938 (1962); **43**, 616 (1962) [English transl.: *Soviet Phys.—JETP* **14**, 1377 (1962); **16**, 442 (1963)]; *Opt. i Spektroskopiya* **13**, 153 (1962) [English transl.: *Opt. Spectry.* **13**, 87 (1962)].

<sup>6</sup> G. H. Wannier, *Phys. Rev.* **90**, 817 (1953).

<sup>7</sup> K. Omidvar, *Phys. Rev.* **140**, A26 (1965).

<sup>8</sup> A. Temkin, *Phys. Rev. Letters* **16**, 835 (1966).

<sup>9</sup> Recent studies by K. Omidvar, *Phys. Rev. Letters* **18**, 153 (1967) are the exception. Not only has Omidvar been able to reproduce the total cross section theoretically with a good degree of accuracy, but in the vicinity of threshold, he has been able to derive a threshold law which in many respects is similar to our results. His absolute magnitude, however, is in error. *Note added*

*in proof:* Because of an error in the phase of the analytic continuation of the hypergeometric function, the cross section reported by Omidvar is in error. However, the analytic form of the cross section near threshold does not change, only the coefficients.

<sup>10</sup> W. L. Fite and R. T. Brackmann, *Phys. Rev.* **112**, 1141 (1958).

<sup>11</sup> A. Boksenburg, thesis, University College, London, 1960 (unpublished). Data taken from a compilation prepared by L. F. Kieffer, JILA Report No. 30, 1965 (unpublished).

<sup>12</sup> E. W. Rothe, L. L. Marion, R. H. Neynaber, and S. M. Trujillo, *Phys. Rev.* **125**, 582 (1962).

<sup>13</sup> J. Wm. McGowan, E. M. Clarke, H. P. Hanson, and R. F. Stebbings, *Phys. Rev. Letters* **13**, 620 (1964).

<sup>14</sup> J. Wm. McGowan, E. M. Clarke, and E. K. Curley, *Phys. Rev. Letters* **15**, 917 (1965); **17**, 66E (1966).

<sup>15</sup> J. Wm. McGowan, *Phys. Rev. Letters* **17**, 1207 (1966); also *Phys. Rev.* **156**, 165 (1967).

<sup>16</sup> J. Wm. McGowan (unpublished).

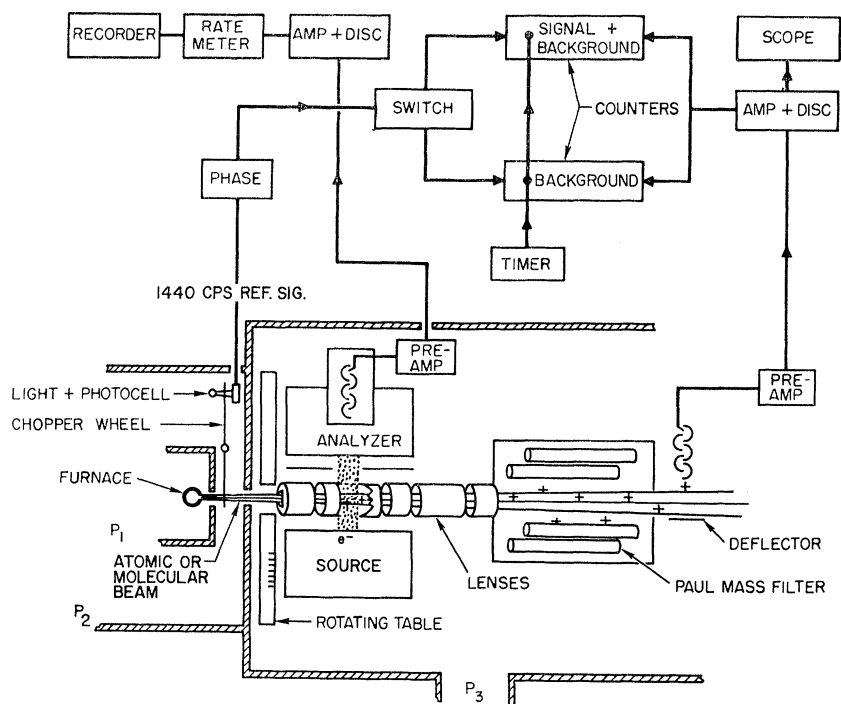


FIG. 1. A diagram of the three-chamber beam machine and of the main electronic equipment used in collecting and recording the experimental data.

Therefore, the description is detailed. In Sec. II, we discuss the following: The electron spectrometer and apparatus used; the method of measuring the electron-energy resolution and of calibrating the energy scale; the determination of ion-collection efficiencies; and our general experimental procedure. In Sec. III, we summarize what is now known experimentally about electron-impact ionization of atomic hydrogen.

## II. APPARATUS, CALIBRATION, AND PROCEDURE

### A. General Description

The experiments described involve the crossing of energy-analyzed electrons with a modulated beam of atoms or molecules. A schematic diagram of the apparatus and of some of the auxiliary equipment is shown in Fig. 1. The ions which are produced in the interaction region receive some momentum from the bombarding electron but continue to travel in a direction essentially that of the original neutral beam. They are subsequently accelerated into a Paul mass filter and analyzed. Those passing through the filter are deflected onto the first dynode of an open-faced electron multiplier and counted. Normally, the density of the particles in the neutral beam at the point where the electron and neutral beams cross ranges from  $10^9$  to  $10^{10}$  particles  $\text{cm}^{-3}$ , depending on the particular atom or molecule in the beam. This point is  $\sim 15$  cm from the beam source which is in the first of three differentially pumped chambers. In the third chamber, the

experimental chamber, the operating background density is approximately  $10^9$  particles  $\text{cm}^{-3}$ .

Many of the auxiliary parts of the apparatus, i.e., the differentially pumped vacuum tanks, the tungsten furnace (used as the atomic-hydrogen source), the quadrupole mass filter, and the beam equipment, are commonly in use in our laboratory and have been described elsewhere.<sup>10,17</sup> Furthermore, many features of the two electron selectors, i.e., the source and analyzer, which make up a major part of our electron spectrometer, have already been described in the literature.<sup>18</sup>

The cross-section area of the neutral beam is defined by a rectangular slit, 5-mm wide by 3 mm high, a short distance in front of the collision region. The total angular width of the neutral beam is near one degree. The electron beam intersects the wide side of the neutral beam. The dimensions of the defining slit for the electron beam are normally 6 mm parallel to the molecular beam axis by 1 mm across the beam, but a number of other combinations of slit widths here and in the source have been tried from time to time. The effect of this angle upon the energy resolution will be discussed below. Even though the electron beam was optically aligned along the axis and in the center of the neutral beam, provision was made so that from outside the vacuum chamber one can adjust the entire electron spectrometer laterally with respect to the neutral beam entering the experimental chamber. With

<sup>17</sup> B. R. Turner, M. A. Fineman, and R. F. Stebbings, *J. Chem. Phys.* **42**, 4088 (1965).

this freedom, we were able to establish that the shape of our ionization-efficiency curves did not depend on a variation in the interaction volume defined by the intersection of the two beams.

In Fig. 2 we show in more detail the electron spectrometer as seen through the center of the electron selectors and in a plane perpendicular to the neutral-beam axis. The selecting and analyzing energy selectors are similar to the Marmet-Clarke-Kerwin selectors.<sup>18</sup> They are 127-deg electrostatic-velocity selectors in which the analyzing field is developed between the outside and inside grids  $G_0$  and  $G_i$ , while the plates  $P_0$  and  $P_i$  are biased such that those electrons which penetrate the grids are collected on the plates. The electrons are analyzed at an energy near 0.5 eV and are post accelerated into the collision region. The electron-energy distribution is measured by swinging the analyzing selector into the electron beam so that those electrons which have traversed the source region can be decelerated and then analyzed as close to the energy at which they enter the source, i.e.,  $\sim 0.5$  eV. If the current is small it is measured with an open-faced electron multiplier. The analyzer is mounted on a disc which can be rotated through an angle  $-95$  to  $+35$  deg with respect to the electron beam.

Although not shown in Fig. 2, electron lenses, electrostatic alignment plates, and collimating slits are sometimes used in the filament region, and immediately preceding and following the collision chamber.

Gold black<sup>19</sup> is deposited on all surfaces which see electrons. The deposition of gold black is important for two reasons: First, it minimizes the reflection of low-energy electrons; second, and perhaps more important, it is an easy to apply, uniformly conducting surface. In our experiments, a polished gold or baked "alki-dag" (colloidal carbon) surface has always been less satisfactory. Apparently, no matter how hard one tries to maintain a deposited gold or dag surface and to keep it clean from finger oils, etc., one usually fails. However, gold black, because it is sooty, visually shows even the slightest abuse. As yet there has been no indication that a finely dispersed gold-black surface charges under electron bombardment.

Under normal operating conditions and with an energy resolution of  $\leq 0.06$  eV, the electron current is less than  $5 \times 10^{-8}$  A. A single run of an ionization-efficiency curve (interval  $\leq 1$  eV) may last more than two hours, during which time the electron-beam current must remain constant to within  $\pm 1\%$ .<sup>20</sup> The data which do not meet this condition are not used, even if, as in the case of our study of diatomic molecules, they

<sup>18</sup> P. Marmet and L. Kerwin, *Can. J. Phys.* **38**, 787 (1960); C. E. Brion, *J. Chem. Phys.* **40**, 2995 (1965); G. J. Schulz, *Phys. Rev.* **125**, 299 (1962).

<sup>19</sup> J. Wm. McGowan, *Rev. Sci. Instr.* **38**, 285 (1967).

<sup>20</sup> In this present apparatus a spectrum is taken in less than 20 minutes and this current stability requirement is  $+1\%$ . Many spectra are then taken and summarized together with a computer.

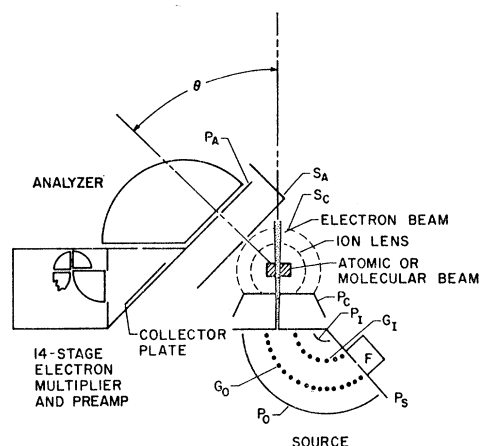


Fig. 2. A slice through the collision region shown in Fig. 1. Shown in the figure are the source and analyzing 127 deg electrostatic electron selectors, the collision region, and some of the shielding in the collision region. The potential difference between the inside and outside analyzing grids  $G_i$  and  $G_0$  is typically 1.05 V. The potentials on the electron collector plates  $P_i$  and  $P_0$  used to disperse space charge in the selector are adjustable between 0 and 40 V. The electric-field free collision region is defined by  $P_c$  and a number of shields including  $S_c$  and  $S_a$ . Although not shown in the figure, additional electrostatic lenses are at times used in the filament region and between  $P_s$  and  $P_c$ . The analyzer may be rotated from  $-95$  to  $+35$  deg.

exhibit all structural features. The prime reason for discounting these data stems from the observation that large electron-current fluctuations are accompanied by measurable shifts in the electron energy. This implies varying conditions in the source selector, apparently in the filament region, which give rise not only to current changes but to slight energy shifts as well. Our most recent design of the electron gun supplying the source selector minimizes these effects. Originally the filament was immediately next to the entrance slit of the source selector. Now, the filament is removed by nearly 3 cm from the entrance slit and electrons are first accelerated to  $\sim 20$  V and decelerated and focused onto this slit by a lens system, which is the slit analogue to the cylindrical lens used to focus the ions into the Paul mass filter.

## B. Electron-Beam Energy and Spatial Distribution

The shape of the electron-energy distribution produced by one selector and sampled by the other is very nearly Gaussian as demonstrated by the trace of recorded distribution shown in the left-hand corner of Fig. 3. Because we have no reason to believe that the source selector and analyzer selector do not both give similar distributions, we expect from the nature of the Gaussian function that the measured energy full width at half-peak height is

$$\Delta = (\Delta_s^2 + \Delta_a^2)^{1/2},$$

where  $\Delta_s$  and  $\Delta_a$  refer to the actual energy widths at half-height for source and analyzing selectors.

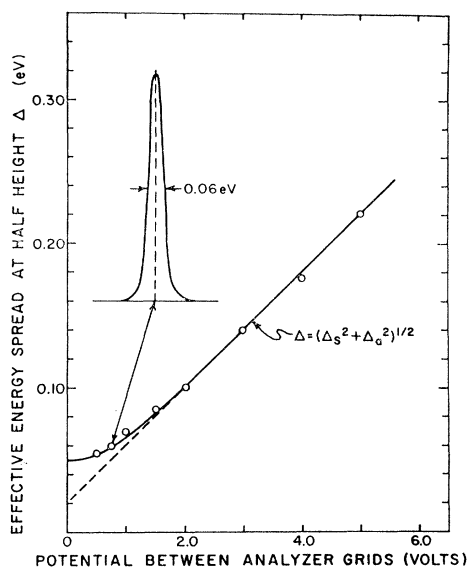


FIG. 3. The energy resolution of the electrons or the effective-energy breadth at half-maximum peak height as a function of the field in the analyzing selector. The field in the source selector is kept constant. The measured distribution is indistinguishable from a Gaussian distribution.

To demonstrate this and to determine experimentally the actual resolution of the electron selectors, we fixed the electric field in the source selector, thereby setting  $\Delta_s$ , and then varied the field in the analyzer. The results are plotted in Fig. 3. They agree very well with our assumed dependence of the measured resolution. The nonlinear extrapolation to zero field in the analyzer gives the energy resolution of the source selector, in this case 0.05 eV. Often  $\Delta_s$  found in the center of the electron beam was  $\Delta_s \approx 0.04$  eV.

Particular attention was given to determine the full energy width of all of the electrons crossing the neutral beam and to ensure that there was no abnormal energy tail on the high-energy side of the electron distribution which might be reflected in our results as low-energy tailing in our ionization curves. Since the electrons coming from the source are energetically anisotropic, it is not sufficient to measure the energy distribution. Rather, it is necessary to measure it on the sides of the beam and to determine the total distribution by adding the currents on the sides to that in the center. In Fig. 4, we show not only the energy but also the spatial distribution of the electrons as well. Part (a) of the figure shows the geometrical arrangement for this experiment. Although the analyzing selector rotates about the center of the neutral beam, it can be treated as if it were rotating about the entrance slit, as for small angles,  $\theta$  and  $\theta'$  are nearly equal. In part (b) of the figure, we show the energy distribution taken at the center of the spatial distribution and the distributions every 1.0 deg to the left and right of the center. In order to construct the total distribution without including any of the current twice, the curves for the

center,  $\pm 1^\circ$ , and  $\pm 2^\circ$  are added together. The constructed distribution which is still indistinguishable from a Gaussian is given in part (c) of the figure. The total energy width  $\Delta$  through source and analyzer is 0.07 eV which normally for our settings of the potentials in the selector corresponds to  $\Delta_s = 0.05$  eV. The total angular spread of the electrons is  $\pm 1$  deg and the width of the beam at half intensity is  $\lesssim 2$  mm. This width is consistent with probe measurements of the spatial distribution in the interaction region.

The electron-energy resolution of the apparatus is severely controlled by the angle  $\beta$  from the top of the collision chamber slit to the bottom of the slit in the filament region. In our crossed-beam configuration this angle further affects the resolution since, in the laboratory frame of reference, the energy of the electron crossing a well-defined atom beam depends not only upon the energy of the atoms and electrons in the beams but also upon the cosine of the angle between the beams, i.e.,

$$4\left\{\frac{m_e}{m_H}E_e E_H\right\} \times \frac{1}{2} \cos\beta.$$

In our experiments the excursion of the electron beam from the electron-beam axis has been as small as  $\pm 1.5^\circ$  and as large as  $\pm 2.5^\circ$ . In the case of atomic hydrogen a generous estimate of the contribution of electron-beam dispersion and the neutral-beam thermal distribution to effective electron-energy distribution is  $< 0.008$  eV.

Besides measuring the energy distribution directly, we have estimated it from the measured breadth of the first elastic scattering resonance in He (19.3 eV) and H (9.56 eV). This gives an upper limit to the energy distribution, but tells us little about the tailing of the distributions used.<sup>14</sup> Using this technique, we have found that the measured breadths are as narrow as 0.04 eV. Also, we have taken the breadth of the structure due to auto-ionization in the first-derivative ionization-efficiency curves for  $O_2$ ,<sup>14</sup>  $N_2$ ,<sup>2</sup> to further check the upper limits to the energy breadth. Finally, in the case of  $H_2^+$ , we have shown that by unfolding different assumed energy distributions of increasing breadth from our experimental data,<sup>21</sup> the peaks in the first-derivative ionization-efficiency curve sharpen. As the process is continued, a point is reached at 0.08 eV where an attempt to remove a broader energy distribution leads to nonsense. This point we take as another indication of the maximum possible energy distribution.

Extreme care had to be taken to make sure that both dc magnetic, and rf fields from the Paul filter, did not destroy our resolution. A degaussed soft iron cylinder was originally used to shield against the earth's field in our earliest measurements. Now a hydrogen annealed degaussed Moly-Permalloy shield is used for this purpose.

<sup>21</sup> H. P. Hanson and Dr. R. Pohler (unpublished); R. F. Stebbings, J. Wm. McGowan, and R. A. Young, NASA Report NAS 59110, 1966 (unpublished).

The rf shielding has proved to be the more serious problem, particularly at 7 Mc/sec. Not only is it necessary to doubly shield all rf leads and the Paul filter, it is necessary to rf ground all dc leads with small capacitors as close as possible to the interaction region. With these precautions the rf field does not broaden the energy distribution more than 5%.

To summarize, the total energy distribution measured in our experiments, with the effect of the spatial distribution included, does not exceed 0.06 eV. When the rf generator is on, the distribution can be broadened by as much as 0.003 eV. Furthermore, the maximum contribution to the effective distribution from the angular dispersion of the beam along the length of the selector slits and from the energy distribution of the neutral beam is now less than 0.005 eV. Therefore, the maximum possible width, due to combined effects of the electron-energy distribution, spatial distribution, and rf broadening cannot exceed 0.07 eV, but 0.06 eV is thought to be a better upper limit for most cases.

### C. Calibration of the Electron-Energy Scale

Although it is possible to determine the electron energy to within 0.1 eV from the characteristics of the apparatus, it is more accurate to calibrate the energy scale by using the appearance potential of some known process as a reference. For experiments already reported, we chose as our reference the ionization potential of atomic hydrogen, 13.595 eV, which in the laboratory frame of reference is 13.602 eV. The energy scales used in the past were based upon the assumption that the ionization-efficiency curve for H(1s) was linear, and that the energy axis intercept could be set at 13.60 eV. However, in this paper, we give evidence that the ionization-threshold law is not linear close to threshold (i.e., for  $\sim 0.4$  eV above threshold), although at higher energies it appears to be so. We further show that the threshold is  $\sim 0.03$  eV below the linear extrapolation point.

For this report we are using the appearance potentials of two previously studied processes to "calibrate" the energy scale. The first reference is the position of the lowest electron scattering resonance in the  $e$ -H system. In earlier papers<sup>14,15</sup> where we had used the linear extrapolation of the H-atom ionization-efficiency curve to fix our scale, we found the measured position to be consistently below the calculated position. The calculated position has now been determined, by a number of theoretical studies under many approximations,<sup>14,15</sup> thus giving us confidence in its validity as an energy reference. The second reference is the structure in the photoionization-efficiency curve, which in the accompanying paper<sup>2</sup> is compared with the first-derivative electron-impact ionization spectrum. The best fit of the structures in the two ionization-efficiency curves gives the same energy reference as above to within  $\pm 0.01$  eV,

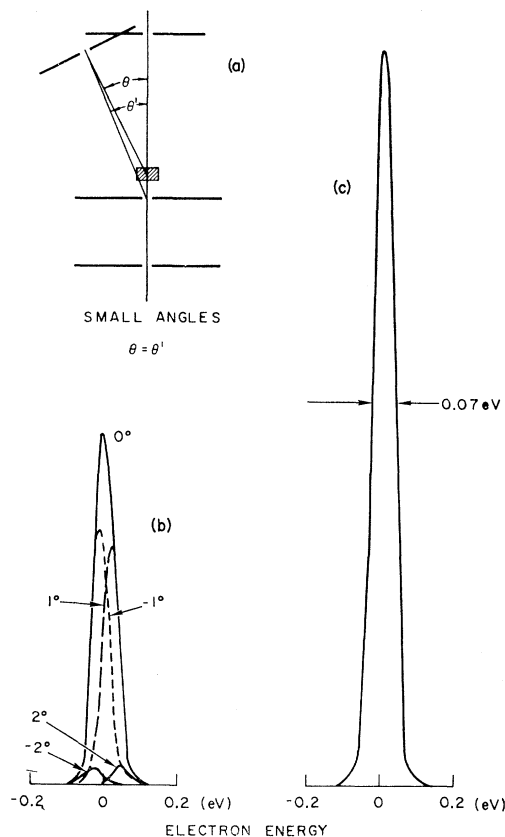


FIG. 4. The measured energy and spatial distribution of the electron beam. (a) A sketch of the geometry for this measurement; (b) the energy distribution at  $\theta=0\pm 1.0, \pm 2.0$  deg; (c) the distribution of all electrons. It is the sum of the curves in part (b) of the figure.

which reflects only our lack of reproducibility from one run to another.

### D. Collection of Positive Ions

Ions formed in the interaction region are already moving toward the cylindrical ion-focusing lens of the Paul mass filter because of the momentum originally possessed by the beam particles. However, the colliding electron imparts some lateral momentum to the resulting ion.<sup>22</sup> Near the threshold, the amount of momentum transferred to the product ion from the electron changes with energy, so that it is necessary to collect with uniform efficiency all the ions or a constant fraction of them as they leave the interaction region. When a potential is applied to the first lens element, the field produced must be strong enough to guarantee uniform collection efficiency as the electron energy is increased, yet weak enough so that it does not penetrate into the interaction region and change the energy distribution of the ionizing electrons and distort the ion trajectories.

<sup>22</sup> W. E. Lamb and R. C. Rutherford, Phys. Rev. **79**, 549 (1950); and R. F. Stebbings, W. L. Fite, D. G. Hummer, and R. T. Brackmann, *ibid.* **119**, 1939 (1960).

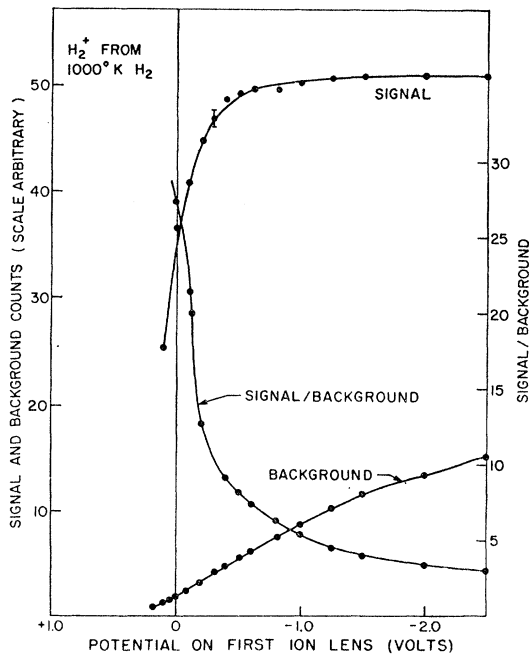


FIG. 5. An analysis of signal and background counts, as a function of the potential on the first ion lens relative to that on the lens elements defining the collision region. The ionizing electron energy was set approximately 0.1 eV above the ionization threshold.

By examining the properties of the cylindrical lens,<sup>23</sup> it is possible to show that under our experimental conditions, the potential on our ion lens produces no measurable effect upon the bombarding-electron energy distribution. Under normal operating conditions, the potential on the first lens for  $H^+$  ions is  $-1$  V, while that for  $H_2^+$  ions is  $-2$  V. Potentials as low as  $-8$  V have been used with no detectable change in the results.

But what of the ion-collection efficiency? In Fig. 5, we examine the case of the collection efficiency for  $H_2^+$  ions from  $H_2$  which has been heated in the tungsten furnace to  $1000^\circ K$ . In this case, the ionizing electron energy was set  $\sim 0.10$  eV above the ionization threshold. As the potential on the first lens becomes more negative (attracting positive ions), the ion current saturates below a potential of  $-2$  V, but at the same time the background counts increase by 150%, because a larger fraction of the ions which are formed from the background  $H_2$  are guided into the analyzer. Consequently, the signal-to-background ratio has decreased by more than a factor of two. To help minimize penetration and to keep the signal-to-background ratio high, we choose to keep the ion drawout potential such that the ion current collected is in the vicinity of 95% of the total current at saturation. Furthermore, it should be clear that 100% saturation and 100% collection efficiency are not necessarily synonymous. In our experiments,

<sup>23</sup> K. R. Spangenberg, *Vacuum Tubes* (McGraw-Hill Book Company, Inc., New York, 1948).

the lack of complete saturation was not judged to be serious, since we were primarily interested in relative measurements. A series of experiments similar to those described above was performed for various electron energies in the threshold region. These demonstrated that the drawout potential did not affect the structure in the  $H_2^+$  ionization-efficiency curves nor the tailing at threshold of  $H^+$  ionization.<sup>2a</sup>

### E. Experimental Procedure

Our normal procedure in this study was to count one minute for each energy setting; in most instances, the number of energy settings per run did not exceed 100. Two energy increments were employed in these threshold experiments: 0.020 or 0.010 eV. It now appears that even 0.010 eV was not a fine enough energy grid to define clearly the structure observed, particularly in the  $H_2^+$  curves discussed in the next paper. In the future, we plan to reduce the energy steps to 0.005 eV.

During the one minute counting, two signals are measured: One due to the background (B) alone, i.e., while the beam is intercepted by the beam chopper; and the other due to signal plus background (S+B), i.e., while the beam pulse passes through the interaction region. The difference between the two integrated counts is the signal itself. For simplicity, in cases where

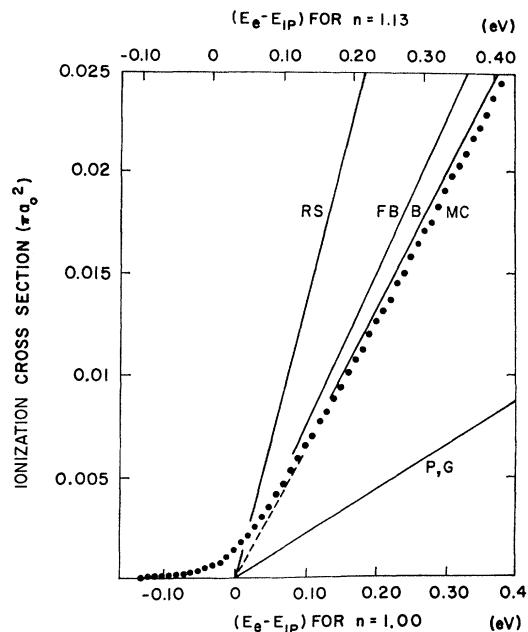


FIG. 6. The cross section for the ionization of atomic hydrogen near the threshold in comparison with other measurements, Fite and Brackmann (FB) and Boksenberg (B) and those theories which predict a linear-threshold law, Rudge and Seaton (RS) and Peterkop (P) and Geltman (G). Part of the tail shown in our experimental curve (MC) is due to the finite-energy resolution of our electron beam. The energy scale judged to be correct is that labeled  $n = 1.13$ . The data have not been smoothed.

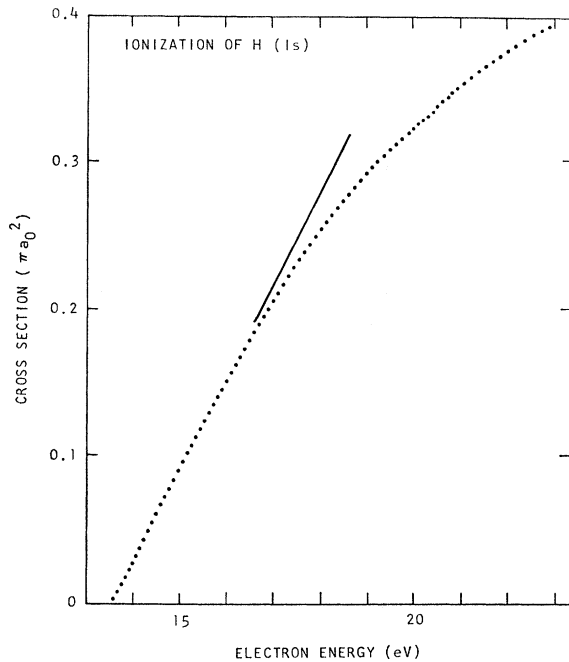


FIG. 7. The measured ionization cross section for 10 eV above threshold showing the near linear portion near threshold.

the signal is much greater than background (e.g., 20/1), we have used (S+B) for our signal as well.

The curves reported in this paper represent the sum of a number of runs. In this way, the statistical errors were minimized and the random errors averaged. At present in the laboratory, a 10-sec counting time is used instead of the one minute originally used. Many more runs are then averaged to give our final experimental data.<sup>20</sup>

### III. RESULTS AND DISCUSSION

#### A. Linear Portion of Curve

Figure 6 shows the absolute cross section for the ionization of atomic hydrogen near threshold. The upper electron-energy scale in the figure is set by the best fit of our data to a 1.13 power law with the electron-energy distribution,  $\Delta_s$ , folded in. The reasons for this will be discussed below. The lower energy scale in Fig. 6 is fixed by setting the linear extrapolation of the straight portion at 13.60 eV.<sup>24</sup> Here it is simply used for comparison of theoretical and experimental results over the linear portion of the ionization-probability curves. The linear extrapolation can also be used as a handy reference point on the energy scale.

The magnitude of the cross section is determined by referring our maximum cross section to that of Fite

<sup>24</sup> Charlotte E. Moore, *Atomic Energy Levels*, Natl. Bur. Std. (U. S.) Circ. No. 467 (U. S. Government Printing Office, Washington, D. C., 1949), Vol. 1. For the energy in the center of mass to be 13.595 eV, the energy of the electrons in the laboratory must be 13.602 eV.

TABLE I. Slopes of the linear portions of the experimental ionization-efficiency curves given in conjunction with several theoretical predictions which derive from a power law,  $(E_e - E_{IP})^{1.0}$ .

	Slope $\pi a_0^2 / \text{eV}$
Experimental	0.064 <sup>a</sup> 0.078 <sup>b</sup> 0.067 <sup>c</sup>
Unweighted Average	0.070 ± 0.008
Theoretical	0.022 <sup>d</sup> 0.136 <sup>e</sup>

<sup>a</sup> See text.

<sup>b</sup> See Ref. 10.

<sup>c</sup> See Ref. 11.

<sup>d</sup> See Ref. 5.

<sup>e</sup> See Rudge and Seaton, Ref. 3.

and Brackmann.<sup>10</sup> Although this measurement does not represent an independent absolute determination of the cross section, it is important because it presents details in the threshold region which are not available from other experiments. Our experimental approach differs from that used by others; and more important, our energy distribution of the electrons is considerably narrower than that employed in the published work.<sup>10-12</sup>

In Fig. 7 the ionization cross section from  $\sim 0.4$  to  $\lesssim 3.0$  eV above the threshold is more like a linear function than a 1.13 power law, but in this region the difference is slight. Figure 6 shows a good agreement between the experimental slopes of the linear segment of the cross section from this work, from that of Fite and Brackmann,<sup>10</sup> and from averaging a number of runs from the thesis of Boksenburg,<sup>11</sup> and it establishes this slope to be  $0.07 \pm 0.01 \pi a_0^2 / \text{eV}$ . The above results and the slopes of linear segments from theory are given in Table I. The slope of the *S*-wave calculation of Peterkop<sup>5,25</sup> is only  $0.022 \pi a_0^2 / \text{eV}$ : This implies that the

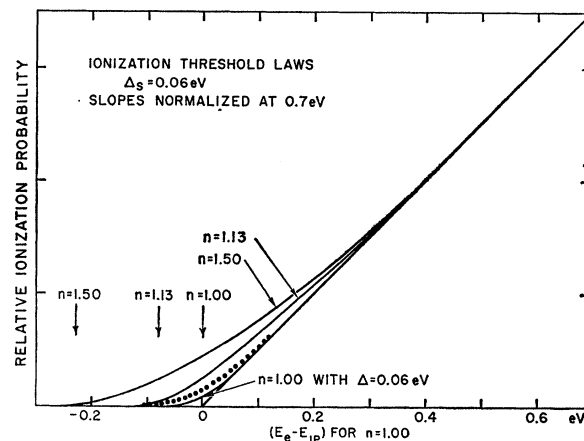


FIG. 8. The ionization of atomic H(1s) with the experimental and calculated probability curves normalized as to slope  $\sim 0.7$  eV above the ionization thresholds. The positions of the curves are then moved relative to the  $n=1$  curve so as to be common with it at 0.7 eV above the linear threshold. There is an obvious disagreement between the experimental results and all threshold laws over such a large interval.

<sup>25</sup> It is with pleasure that we thank Dr. I. J. Kung for pointing out the correct value of Peterkop's *S*-wave calculation of the slope of the ionization cross section.

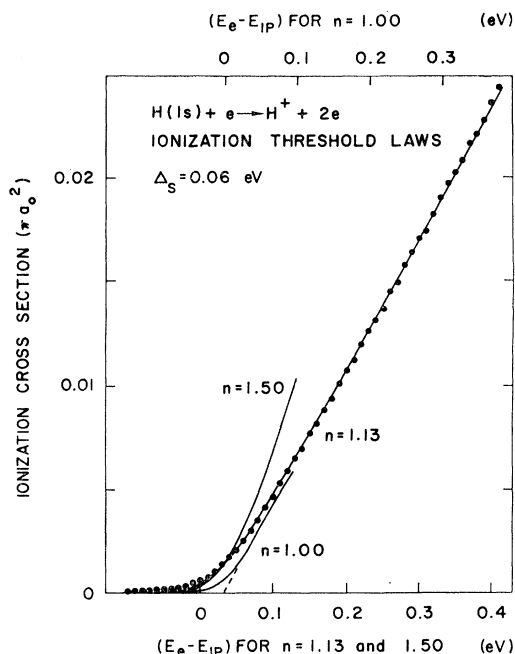


FIG. 9. The measured ionization cross section for  $H(1s)$  near threshold shown in comparison with calculated cross section. In order to obtain a good fit between the calculated curve for a 1.13 power law and the data, the calculated curve had to be displaced in energy from the linear curve by  $-0.032$  eV. It is  $\sim 0.03$  eV which is now recognized as the error one makes in calibration by assuming a linear-threshold law for atomic H ionization. The calculated curve for  $n=1.50$  has also been displaced together with that for  $n=1.13$ . The calculated curve for  $n=1.00$  represents the data at higher energies but not at threshold.

contributions for higher partial waves are of great consequence. The recent calculation by Omidvar<sup>9</sup> is not linear, and lies between the Peterkop and experimental results. The slope of the cross section derived by Rudge and Seaton<sup>3</sup> is  $0.136\pi a_0^2/\text{eV}$  and is too large.

### B. Nonlinear Portion of Curve

Only a portion of the tail shown in the experimental data is due to the finite-energy resolution of the electrons. As was demonstrated, the full width of the Gaussian distribution at half maximum  $\Delta_s$  is less than 0.06 eV. This contribution to the total tailing is shown in Figs. 8 and 9, in which the electron-energy distribution is folded into the linear-threshold law. If the linear-threshold law applied and if the tail were due only to the energy distribution of the electrons, the tailing in our experimental curve would correspond to an energy distribution approaching 0.13 eV. There is no possibility that our electron-energy distribution could be so broad, nor can we associate this tailing with any of the possible instrumental factors, since all estimates of these effects are small and should appear as part of our measured width. We are therefore forced to conclude that the tailing is associated with the ionization process itself. The simplest suggestion is

that in the threshold region, the ionization-probability curve is nonlinear.<sup>26</sup>

Figures 8 and 9 show our experimental results compared with curves for the three simple threshold laws described here. In order to make possible a comparison between theory and experiment, our experimental energy distribution is folded into the theoretical curves in the following way:<sup>27</sup>

$$F(E_e) = |\pi \Delta_s^2 / 4 \ln 2|^{-1/2} \times \int_{-\infty}^{\infty} \exp[-4 \ln 2 (E_e - E')^2 / \Delta_s^2] f(E') dE',$$

where  $\Delta_s$  is the full width of the electron-energy distribution at half maximum intensity, i.e., 0.06 eV and where

$$f(E') = (E' - E_{IP})^n$$

is the functional dependence of the ionization cross section and  $E_{IP} = 13.60$  eV.

Our first attempt to fit the power laws over a large energy interval was not successful as exhibited in Fig. 8. Here we have chosen  $n=1.00$ , 1.13, and 1.50, and we have normalized the slopes 0.7 eV above the ionization thresholds. We have then displaced the  $n=1.50$  and  $n=1.13$  curves so that they overlap the  $n=1.00$  curve and the data. The displacements necessary to overlap the 1.5 and 1.13 power-law curves are  $|\Delta E_{1.5-1.0}| \sim 0.23$  eV and  $|\Delta E_{1.13-1.0}| \sim 0.08$  eV, which are inconsistent with our calibrations of the energy scale, i.e., the position of the lowest ( $e$ -H) scattering resonances and the position of the  $H_2^+$  auto-ionization structure. It follows that a simple power-law dependence cannot be extended 0.7 eV above threshold; although a much better fit can be made over a smaller energy interval as discussed below.

In Fig. 9 we have best fitted the calculated threshold laws for  $n=1.13$  and 1.50 to the lower portion of the experimental curve. Once again we have allowed the energy folded 1.5 and 1.13 power-law curves to be shifted downward in energy; this time  $|\Delta E| = 0.032 \pm 0.005$  eV for both cases. The fit between our data

<sup>26</sup> In a personal communication, O. Bely suggested that some of the tailing in the ionization curve near threshold might be due, in part, to the following: Just below the ionization threshold, the bombarding electrons excite the hydrogen atoms to the higher excitation levels which are very long-lived, i.e., greater than a microsecond. If the excitation cross sections for all levels  $n \geq 16$  behave at threshold like the threshold of  $2p$  excitation, i.e., if it is finite at threshold, then a combination of large cross sections at threshold creates an excited target which can be effectively photoionized by the room temperature blackbody radiation in the vacuum system. A crude estimate of this effect places it within an order of magnitude of explaining our results. It is not likely that more refined calculations can be made, but the system does lend itself to straightforward experimental examination, which we hope can soon be undertaken, even though we now feel the present evidence conclusively shows the ionization probability curve to be nonlinear near threshold.

<sup>27</sup> The constant  $4 \ln 2$  in the following equation was accidentally left out of Eq. (8) of the article by J. Wm. McGowan, Phys. Rev. 156, 165 (1967).



and the calculated curve for the 1.5 power law is poor even over the first 0.04 eV. Above 13.60 eV the two curves diverge rapidly. On the other hand, the fit between the data and the energy-folded 1.13 power-law curve is good over  $\sim 0.4$  eV. Above this the divergence of the curves is slight but evident. Below 13.60 eV the data remain distinctly above the calculated curves. However, in this region, the excess tailing is consistent with a power law  $n < 1.13$  provided the threshold is lowered still further.

It follows directly from the above discussion that the H(1s) ionization cross section, within the limits of our experiment, is linear between  $\sim 0.4$  and  $\leq 3$  eV above threshold. Below  $\sim 0.4$  eV the cross section is nonlinear and approaches a predicted  $n = 1.127$  power law. However, this does not preclude the possibility that even closer to the "undefined" threshold some other law may apply. In short, for the first 3 eV above the ionization potential of atomic hydrogen, the cross section is a complicated function of the electron energy.<sup>28</sup>

Since the completion of our paper, Vinkalns and Gailitis<sup>29</sup> have theoretically studied the ionization-threshold problem. Their approach is similar to that of Wannier<sup>6</sup> and the results they obtained are very similar to our own experimental results.

#### IV. SUMMARY

Considerable evidence has been gathered which suggests that the ionization-threshold law governing the ionization of atomic H (and probably of all atoms and molecules) is nonlinear and complicated in the threshold region. Although it is impossible to derive exactly the threshold behavior from our data, our results over the first 0.3 eV are well described by a  $1.13 \pm 0.03$  power law with our experimental energy

<sup>28</sup> Unpublished measurements of the ionization threshold of He have repeatedly shown a nonlinear and complex dependence of the cross section upon the ionizing electron energy. Recent measurements by C. E. Brion and G. E. Thomas confirm a nonlinear dependence.

<sup>29</sup> I. Vinkalns and M. Gailitis, in Proceedings of the Fifth International Conference on the Physics of Electronic and Atomic Collisions, Leningrad, U.S.S.R., 1967, p. 648 (unpublished); and *Collisions of Electrons with Atoms* (The Physics Institute of the Latvian Academy of Sciences, Riga, 1967), Vol. IV, p. 17. (A translation of this article is available from G. H. Wannier, University of Oregon, Eugene, Ore.)

distribution folded into it. The above is based on the following evidence:

1. The simple  $1.13 \pm 0.03$  power law fits our experimental data over more than 0.4 eV of the threshold region. This results in an effective shift downward of our electron-energy scale by 0.03 eV as compared with a calibration based upon a linear law.

2. Agreement with theory is obtained for the measured position of the lowest  $^1S$  elastic scattering resonance for electrons in H(1s), when the experimental-energy scale is shifted 0.03 eV.

3. The structure observed in the first-derivative electron-impact ionization spectrum of  $H_2^+$  agrees best with the photo-ionization structure when the electron-energy scale is shifted to account for a nonlinear-threshold law.

The 1.13 power-law dependence does not appear to persist for more than 0.4 eV. Above this a linear power law more accurately describes our findings. Finally, through the linear portion of the curve, all of the experiments reported agree as to the slope of the linear portion of the ionization cross section just above threshold. The average slope one obtains from three experiments is  $(0.070 \pm 0.008)\pi a_0^2/\text{eV}$ , which lies between the various theoretically predicted values. Additional work in our laboratory is planned to verify and extend these findings.

#### ACKNOWLEDGMENTS

It is with great pleasure that we express our appreciation to the many who have thought with us about the problems discussed in this report. We would like to thank in particular O. Bely, G. H. Dunn, S. Geltman, L. J. Kieffer, K. Omidvar, and A. Temkin for discussions on ionization of atomic hydrogen. Correspondence with M. Gailitis is appreciated. Our thanks goes particularly to M. A. Fineman and H. P. Hanson who contributed to the early portions of this work and to the members of the Atomic Physics Laboratory who, under various directors W. L. Fite, R. F. Stebbings and D. M. J. Compton, make a sizeable contribution to our program. Particular recognition must go to Aage Kristensen for his help in and imagination given to the construction of our apparatus.